Vehicle-to-grid charging control strategy aimed at minimizing harmonic disturbances

Mikel González[1] ; Francisco Javier Asensio[1] ; José Ignacio San Martín[1] ; Inmaculada Zamora[2] ; José Antonio Cortajarena[3] ; Oier Oñederra[2]

[1]Department of Electrical Engineering, Engineering School of Gipuzkoa, University of the Basque Country, Avda. Otaola 29, 20600 Eibar (Spain)

[2]Department of Electrical Engineering, Engineering School of Bilbao, University of the Basque Country, Plaza Torres Quevedo 1, 48011 Bilbao (Spain)

[3]Department of Electronical Technology, Engineering School of Gipuzkoa, University of the Basque Country, Avda. Otaola 29, 20600 Eibar (Spain)

Correspondence
Francisco Javier Asensio (e-mail: franciscojavier.asensio@ehu.eus)

Funding information
Spanish Ministry of Universities (FPU19/01902), Basque Government (GISEL Research Group IT1191-19, PIBA_2019_1_0098 and ELKARTEK KK-2020/00050) and the University of the Basque Country UPV/EHU (COLAB19, PIFG19/12 and PIF19/173)

Summary
This paper presents the design and implementation of a control for an electric vehicle charger to provide Vehicle to Grid (V2G) services while reducing the current Total Harmonic Distortion (THD). The control is composed of two current loops. The main one controls the active and reactive powers in a decoupled way, and the second one, focuses on the reduction of the 5th order harmonic component. After explaining the mathematical modelling, the methodology and the experimental setup, the results of the experimental validation are shown. Several experiments were conducted on a scale-based charger connected to a 400V grid to observe the performance of the proposed control. Results have shown that the developed control enhances the power quality by reducing the 5th harmonic component by 76.34%, and hence, the current THD from 6.06% to 2.82% and that can successfully provide voltage and frequency regulation without adding extra weight or volume. The proposed strategy can also be extrapolated to other harmonic orders; therefore, it is suitable for grids with high components of certain harmonics.

Keywords
Control design, electric vehicle, fifth harmonic, harmonic distortion, power grids, PWM inverters and V2G.

1 | INTRODUCTION
Global warming is an undoubtable fact which is mainly affected by human activity. Indicators on this regard are periodically reviewed and updated by the Intergovernmental Panel on Climate Change (IPCC), which has concluded that the impact of the rise of global temperature is catastrophic [1]. Consequently, finding effective solutions is a key factor to overcome this problem [2]. In this sense, the regulatory framework of the European Union for 2030 proposes an energy transition towards a cleaner model, based on renewable generation sources, as set out in the package of measures known as "Clean Energy for All Europeans" [3].

Besides, the EU goes a step further by aiming to have a sustainable economy and to be carbon-neutral and by 2050 [4]. Nevertheless, renewable energies have a series of associated problems that need to be addressed, like uncertainty, surplus power production, bidirectional power flows, loss of the inertia of the grid which lead to faster dynamics, etc. [5]-[7] So, provision of ancillary services to overcome the above mentioned problems is essential [8]. In this sense, the Electric Vehicle (EV) is a promising technology for decarbonizing the transport sector [9]. However, in case they are integrated in an inappropriate way, they can generate some issues on the transmission lines and power transformers [10]-[12].

This context is an excellent breeding ground for the development of control architectures and topologies that will allow developing Vehicle-to-Grid (V2G) applications [13]. Apart from launching new economic opportunities [14], V2G will enable the integration of renewable energies in a massive way. Furthermore, with an appropriate recharging

strategy, V2G can also overcome the problem of lines overloading [15], [16]. In addition, it can provide ancillary services such as peak levelling, load balancing, frequency regulation, voltage regulation, etc. [17]-[21]. In this regard, EVs remain parked around 96% of the time, which favors the provision of V2G services [22]. However, such services increase the induced degradation on batteries, which should be considered to ensure the viability of the V2G [23]-[25]. Among others, this degradation is influenced by the temperature, the State of Charge (SOC) of the batteries, the current ratio used during charging and discharging, the Depth of Discharge (DoD), etc. [26], [27]. So, a proper control for EV chargers is needed to reduce the induced degradation of the batteries [16], [28].

In this new power grid scenario with more and more integrated nonlinear loads, higher harmonic distortion is becoming remarkable, which have negative effects on the power system [29], [30]. EV chargers are also nonlinear loads, and hence an important source of harmonics [31], [32].

In the current literature of the EV chargers field, many research works focused on harmonic reduction or elimination have been proposed [33]-[38]. After analyzing the different methods, it can be said that passive filters, Artificial Intelligence (AI), Active Power Filters (APF), and Selective Harmonic Elimination (SHE) are the most relevant and used ones.

Regarding the use of passive filters for current THD reduction, they commonly involve a high cost, weight and volume of the system. Besides, if they are not well designed, they could lead to resonance problems [39]. Total Harmonic Distortion (THD) can also be reduced by increasing the current loop gain of an EV charger control, but this can compromise the stability of the charger controller [40].

In case of using AI-based controllers, they ensure a fast dynamic response and do not compromise system stability. Nonetheless, they require a lot of time and effort to be implemented in order to avoid the overfitting of the data while maintaining a good accuracy [41]-[44]. For the case in which EV chargers are used as APFs [45]-[48], they success in reducing harmonic content but they also involve a high development cost, even more if they are designed for both reducing harmonics and giving grid support [49], [50].

Many control strategies focus on Selective Harmonic Elimination (SHE) algorithms [51]-[54], but most are based on multilevel converters, which despite their better harmonic response are more expensive in cost, and require more volume and weight as they consist of more elements [55].

In this scenario, analyzing the aforementioned methods it can be said that they are either too complicated to implement or require additional devices that make the installation more expensive, larger, and heavier. Besides, considering an electrical grid with voltage harmonics, the current injected by the EV converters will contain additional harmonics. This effect is increased if one of the grid harmonics is particularly high [56]. In this sense, there is a lack in the current literature about a specialized and a low-cost method for reducing a specific harmonic considering the already existing harmonics in the grid.

Considering all the above mentioned, this paper proposes a control strategy aimed at reducing the current THD produced by a specific voltage harmonic of the grid. In comparison of the already existing methods in the field of EV chargers, this control strategy is simple to implement, robust, and does not require additional elements. The control scheme consists of two current loops, the main one allows an independent control of the active and reactive power, and the second one suppresses the n^{th} harmonic of the current. For this case, the proposed control strategy has been used to develop a Fifth Harmonic Controller (FHC) to suppress the fifth harmonic.

The structure of the paper is as follows: in section 2 the mathematical models of the system, the control, the converter and the modulation are shown; in sections 3, the proposed control strategy and the experimental setup are explained. In section 4 the experimental results are displayed. Finally, in section 5, main conclusions are shown.

2 | MATHEMATICAL MODELLING

In this section, all the mathematical bases necessary to model the system and all its components have been exposed. First, the equations that govern a grid-connected VSC system have been explained. Then, the traditional control is obtained. Finally, the model of the inverter has been obtained and the SVPWM technique to modulate the control signal has been explained.

2.1 | Grid-connected VSC system

The system is composed of three main elements (converter, RL filter and grid) and the control, as it can be seen in Fig. 1.

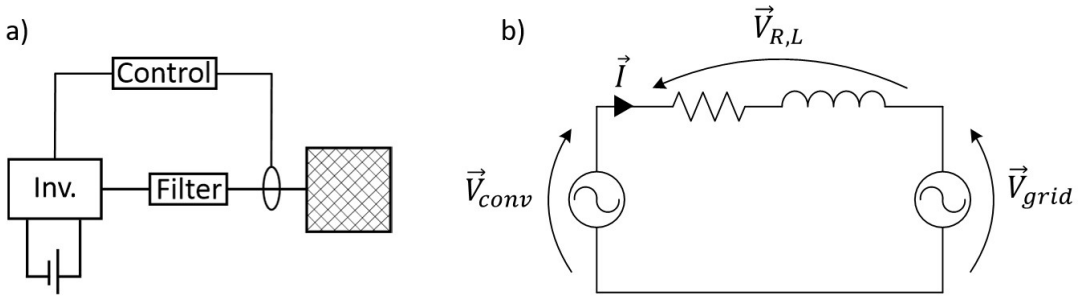

FIGURE 1 Inverter connected to the grid with a RL filter. a) General scheme of the system. b) Electric scheme of the system.

Considering the voltage balance of the three elements, (1) is obtained.

$$\vec{V}_{conv} = R \cdot \vec{I} + L \cdot \frac{d\vec{I}}{dt} + \vec{V}_g \quad (1)$$

Where $\vec{V}_{conv}$ [V] denotes the output voltage of the inverter, R [Ω] and L [H] the resistive and the inductive components of the filter respectively, $\vec{I}$ [A] refers to the current injected to the grid and $\vec{V}_g$ [V] the voltage of the grid.

By using the Clarke and Park transforms, equation (1) is transformed from a static three-phase reference frame ("abc") to a rotating two-phase frame ("dq"). With this, three sinusoidal components are transformed into two direct current components. Then, if the real part and the imaginary part are separated, and the Laplace transform is applied to each of them, the result is (2) and (3).

$$I_d = \frac{V_{convd} - V_{gd} + \omega \cdot L \cdot I_q}{R + s \cdot L} \quad (2)$$

$$I_q = \frac{V_{convq} - V_{gq} - \omega \cdot L \cdot I_d}{R + s \cdot L} \quad (3)$$

Where "d" and "q" subscripts are used for expressing the direct and the quadrature axis, respectively, of the "dq" reference frame, whereas s is the symbol for Laplace operator and ω [rad/s] is the angular frequency of the grid voltage.

Equations (2) and (3) represents the behavior of the converter-filter-grid system. Both equations show that I_d and I_q are coupled, and thus, they are dependent variables. In other words, they cannot be controlled separately.

2.2 | Traditional control

The objective of traditional current control is to achieve independent control of active power (P) and reactive power (Q). To do so, the first step is to define their formulas in the "dq" reference plane, (4) and (5) respectively [57]:

$$P = \frac{3}{2}\left(V_{gd} \cdot I_d + V_{gq} \cdot I_q\right) \quad (4)$$

$$Q = \frac{3}{2}\left(V_{gq} \cdot I_d - V_{gd} \cdot I_q\right) \quad (5)$$

To achieve the above-mentioned independent power control, the active power must be left only as a function of I_d and the reactive power as a function of I_q. For this purpose, by using a Phase-Locked Loop (PLL), the "d" axis of the "dq" plane is aligned to the vector $\vec{V}_g$. In this way, the V_{gd} component will have the value of the modulus of V_g, and V_{gq} will have a value of zero. Thanks to this, the active power is just a function of I_d, and the reactive power is simply a function of I_q [58].

As can be seen in equations (2) and (3), I_d and I_q are interdependent. Therefore, a decoupling must be added to the current control. This decoupling allows to unlink these variables by subtracting the expression $(\omega \cdot L \cdot I_q)$ from I_d, and adding the expression $(\omega \cdot L \cdot I_d)$ to I_q.

Once this has been done, both active and reactive power can be controlled independently by means of a current loop, as shown in Fig. 2 [59]-[63]. Thus, the active and reactive powers can be controlled as a function of the reference signals I_d^* and I_q^*, respectively.

With this loop, an independent control of the active and the reactive powers can be achieved, and, hence, the converter will be able to work in all four quadrants, injecting and consuming both active and reactive power [64].

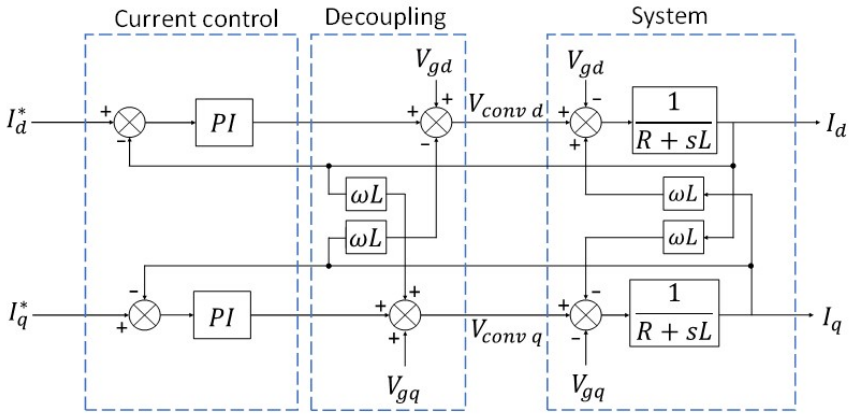

FIGURE 2 Current control of the VSC.

2.3 | Converter

The three-phase two-level Voltage Source Converter (VSC) is widely used because has a simple structure and enables an independent control of the active and reactive powers. Transistors of the same branch cannot be activated at the same time, otherwise they would short-circuit the DC bus. This is why the converter has 8 possible configurations, as shown in Fig. 3 [65]-[67]. Each state of the converter is enumerated with a vector, resulting in six active vectors ($\vec{V}_1$ to $\vec{V}_6$) and two null vectors ($\vec{V}_0$ and $\vec{V}_7$).

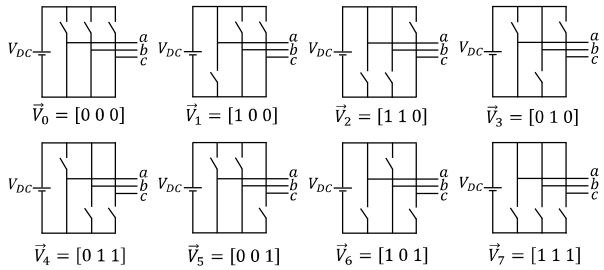

FIGURE 3 Three-phase two-level VSC switching states and their vector.

2.4 | Modulation

The modulation transforms the reference voltage of the control block into binary signals (ON/OFF) to activate and deactivate the inverter transistors, and is normally performed using the Pulse Width Modulation (PWM) technique [68].

Since the SVM technique, also known as SVPWM, makes better use of the DC bus, is one of the most commonly used control techniques for three-phase two-level VSC. Its operating procedure is based on the following steps: first, the control calculates and sends the vector $\vec{V}_{conv}^*$ as a reference. Then, the two adjacent inverter's switching state vectors are identified. Next, it calculates for how long each of the adjacent vectors and the null vectors must be activated. Finally, this information is sent to the VSC transistors throughout the corresponding switching divers.

3 | PROPOSED METHODOLOGY AND EXPERIMENTAL SETUP

Traditional inverter controls, when working in electrical grids with a high component of a specific voltage harmonic, cause the current injected to the grid to be distorted, to a large extent, by this harmonic component of the grid voltage. So, the objective of the proposed methodology is to reduce the THD of the current injected into the grid. The proposed methodology can be adjusted for any harmonic number. For the explanation, it has been decided to tune it to the fifth harmonic, thus obtaining a Fifth Harmonic Controller (FHC).

The FHC scheme consists of two loops, the primary control, and the secondary control. The primary loop is a modified version of the traditional current control which is commonly used to set the desired active and reactive power. The modification involves the elimination of the fifth harmonic component from the measured current. The secondary control is responsible for reducing the distortion that this voltage harmonic generates in the current

In the primary control, the first step is to find the angle (θ) of the grid voltages (V_{ga}, V_{gb}, V_{gc}). For that a PLL is used. Then, the reference plane of the grid currents (I_a, I_b, I_c) is changed from "abc" to "αβ" (static two-phase frame) by applying the Clarke transform. In this "αβ" plane, the fifth harmonic component is removed from the currents using a band-stop filter. Once the fifth harmonic has been filtered out, the reference plane is changed to "dq" plane ($I_d,\ I_q$), where the traditional control of the active and reactive powers is carried out. That is, the references (I_d^*, I_q^*) are compared with the measured currents, the error is introduced into a PI controller, the controller output is decoupled to be able to control independently the active and reactive power and, finally, the references of the "αβ" plane $(V_{conv,\alpha}^*, V_{conv,\beta}^*)$ are introduced into the modulation block. In this block the switching signals (S_a, S_b, S_c) are calculated and sent to the converter.

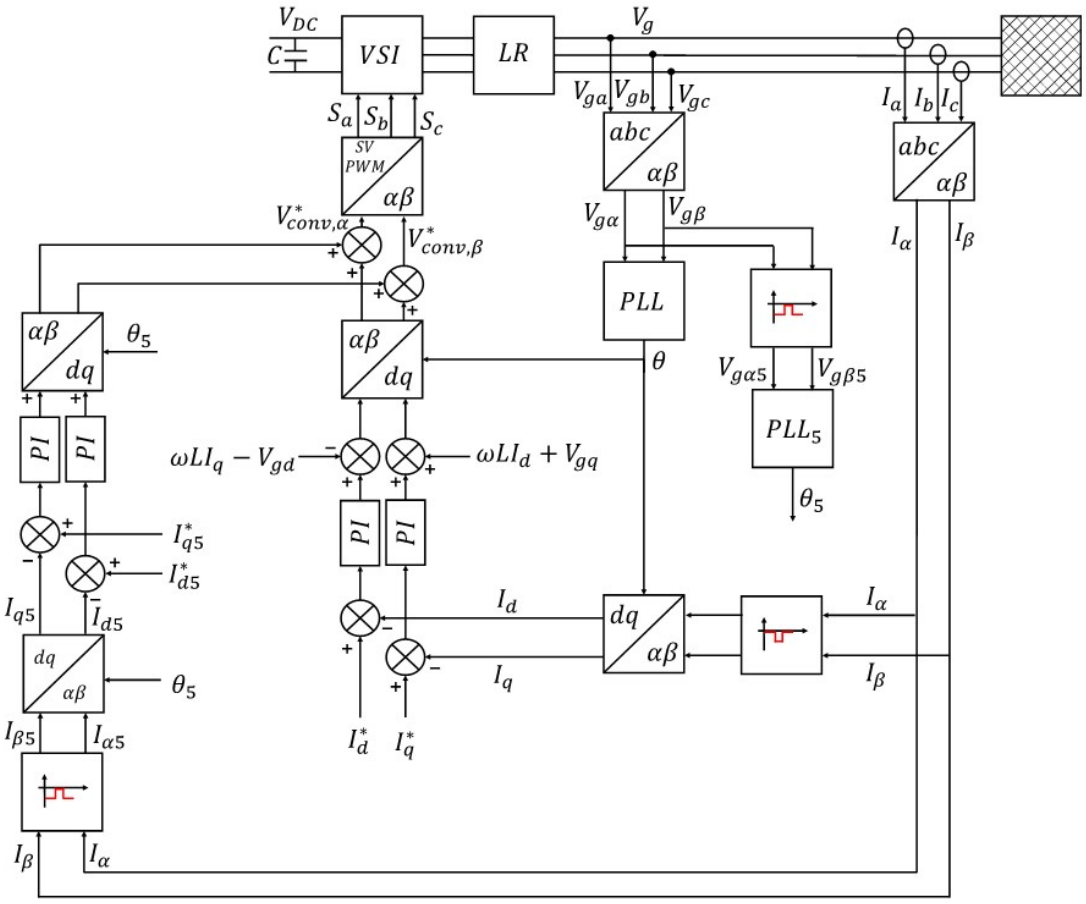

FIGURE 4 Proposed control to reduce current harmonics.

The secondary control works in a similar way to the primary control. First, it measures the corresponding angle of the fifth harmonic of the network voltage (θ_5). For this, a band-pass filter and a PLL set to 250Hz are used. Using another band-pass filter, the components of the fifth harmonic of the current are isolated and transformed to the "dq" reference plane. Then, the references are set to zero $\left(I^*_{d5} = I^*_{q5} = 0\right)$ so that the effect of the fifth harmonic voltage on the current disappears. Finally, after comparing the measured currents with the references and passing the error through the PI controllers, the references in the “αβ” plane are introduced into the modulation block.

Regarding the experimental setup, Table 1 shows the characteristics of the used elements and the conditions under which the experiment was carried out.

TABLE 1 Experimental setup

According to the used elements, the power converter was the Pasaban INF 50-10, with Infineon FS150R12KT4_B11 IGBTs. For the Digital Signal Processor (DSP) and the DC source, dSPACE PX10 Expansion Box and PVS60085MR model from BK PRECISION were used respectively, whereas for the drivers, MONTELEC MTC-3001B.

The laboratory test bench can be seen in Fig. 5.

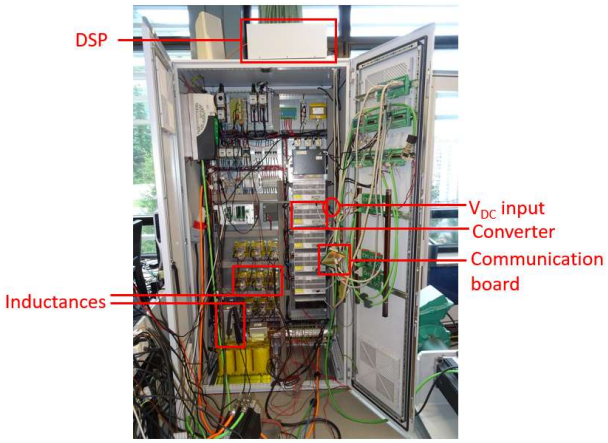

FIGURE 5 Setup of the experiment.

As it can be appreciated, the implementation of this control does not require any additional element compared to the classical control theory, and thus, not extra weight or volume is added.

4 | RESULTS AND DISCUSSIONS

To study the behavior of the FHC control, three experiments have been conducted:

- In the first one, the harmonic response of traditional control and the proposed FHC control have been compared.
- In the second one, the dynamics of the FHC has been analyzed considering a sudden increase in the demand from the grid.
- Finally, in the third experiment, the capacity of the FCH to provide the network with voltage compensation has been studied.

Note: Due to hardware limitations, the experiment could not be conducted in greater power ranges that the ones shown hereafter. The battery has been emulated with the PVS60085MR power supply. This power supply delivers a maximum power of 3kW. Considering that the grid is three-phase 380V, the maximum current that can be injected into the grid is 4.5 A RMS. It is true that the set current has been slightly lower than the maximum current of the power supply, but it has been by no means possible to reach the limit that the inverter allows.

4.1 | Harmonic performance comparison between regular control and the FHC control

In this section, harmonics of the regular control (Fig. 3) and harmonics of the FHC control (Fig. 4) have been compared. To this effect, two trials have been conducted, one with the traditional control of the converter and another one with the FHC control. In both tests, currents have been measured both in the "dq" reference frame and in the "abc" reference frame. These results can be observed in Fig. 6.

As can be seen in Fig. 6, the currents measured follow the imposed references, so it is assumed that both controllers work properly in the steady-state. Also, it can be seen that the currents injected by the FHC have less perturbances than those of the regular control. To quantify this improvement, the Fast Fourier Transformation (FFT) on both injected current has been applied (Fig. 7).

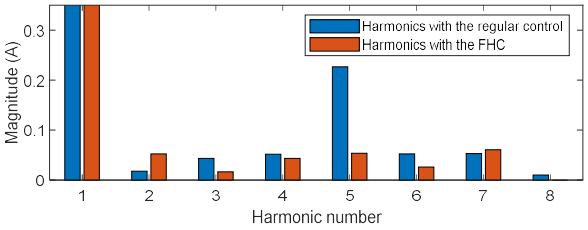

FIGURE 7 Harmonic decomposition of the injected current with the FHC.

Comparing the harmonics of the traditional control and the FHC control, the analysis by FFT shows how the module of the fifth harmonic decreases notoriously, from 0.23A to 0.05A, in other words, it has been reduced by 76.34%. The rest of the harmonics remain practically invariable since the changes are not remarkable. In this sense, after calculating the THD obtained from applying both controls, it can be seen how the FHC reduces the THD from 6.09% (with the regular control) to 2.82%.

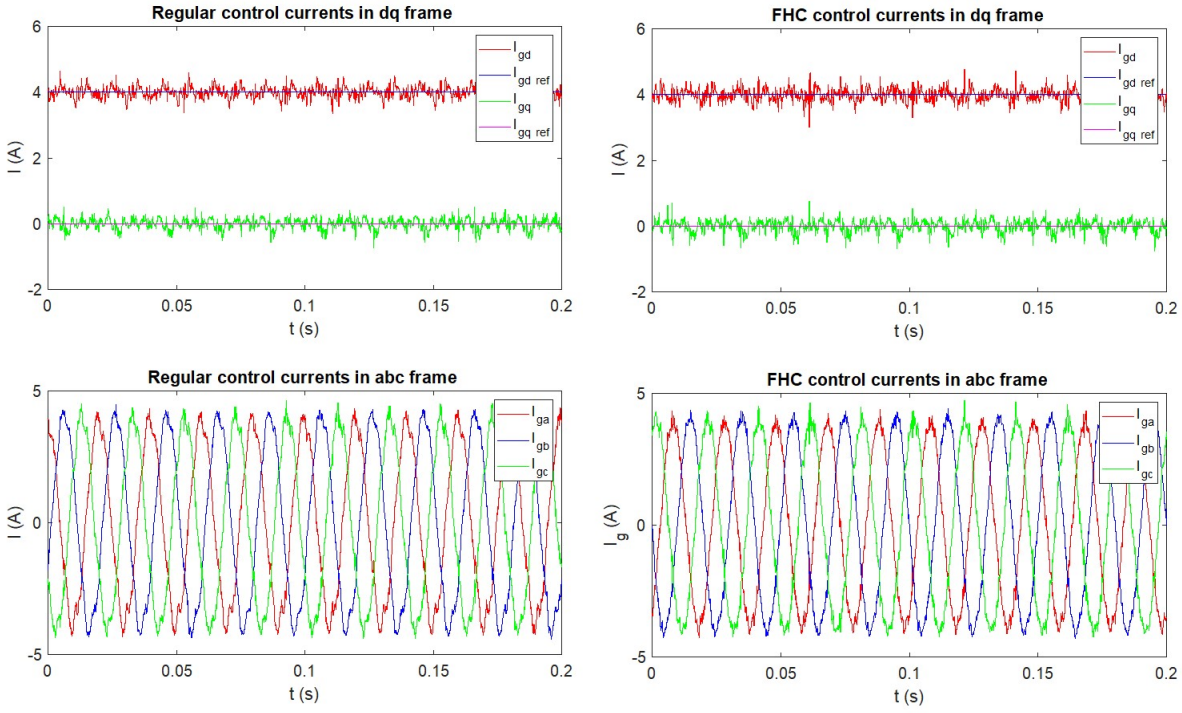

FIGURE 6 Currents in "dq" (up) and "abc" (down) reference frames from both trials, regular control (left) and FHC control (right).

4.2 | Dynamics of the FHC under a sudden variation of the active power demand of the grid

This second experiment aims to analyze the dynamics of the FHC when there is a sudden increase in the demand for active power by the grid. This case simulates a situation where the EV is providing V2G services and there is a drop in frequency in the grid. In this situation, the aggregator will order the EV to immediately provide active power to the grid, and the EV should respond fast.

To recreate that scenario, a 100% step has been introduced in the I_d reference, rising from 2A to 4A, since this component (I_d) is the one that controls the active power. The result of the test can be seen in Fig. 8 and Fig. 9, wherein the first one the currents are shown in the "dq" reference frame, and in the second one, in the "abc" reference frame.

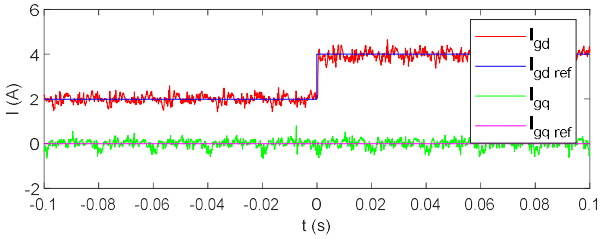

FIGURE 8 References and measures I_{gd} and I_{gq}.

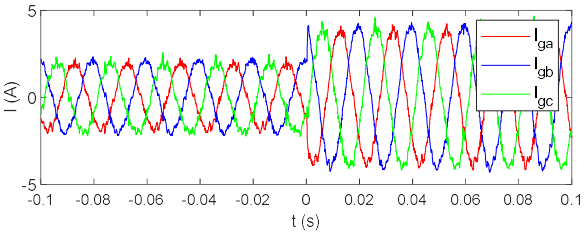

FIGURE 9 Injected currents to the grid.

In Fig. 8 it can be seen that the measured current is adjusted to the value of the imposed current. Furthermore, the system response time is approximately 1ms, having an absolute maximum error of 0.06A and a relative maximum error of 15%. From this, it can be concluded that the dynamics of the controllers are appropriate.

4.3 | Reactive power with the FHC

To provide the grid with voltage compensation, it is necessary for the EV to be able to exchange reactive power with the grid in a bidirectional way. To study how the FHC does this, two laboratory tests have been performed.

- Injection of reactive power to the grid by imposing $I_d = 3A$ and $I_q = 3A$. Thus, a leading power factor is obtained (capacitive).
- Consumption of reactive power from the grid by imposing $I_d = 3A$ and $I_q = -3A$. Thus, a lagging power factor is achieved (inductive).

The results from these two tests can be seen in Fig. 10 and Fig. 11, respectively.

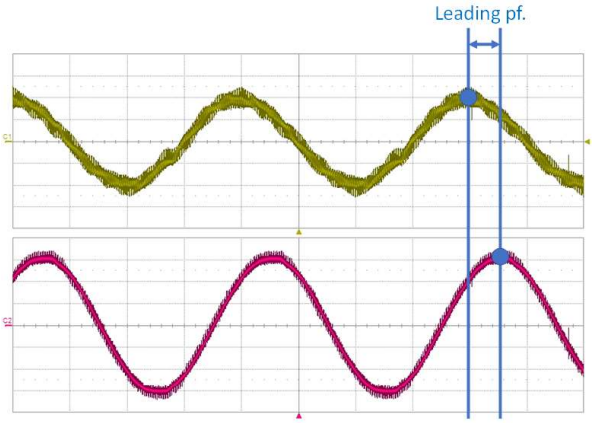

FIGURE 10 Leading power factor. Up: current (y axis, 2 A/box) vs time (x axis, 5 ms/box). Down: voltage (y axis, 100 V/box) vs time (x axis, 5 ms/box).

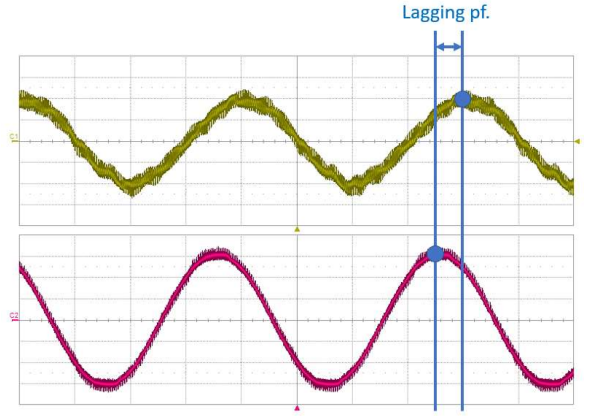

FIGURE 11 Lagging power factor. Up: current (y axis, 2 A/box) vs time (x axis, 5 ms/box). Down: voltage (y axis, 100 V/box) vs time (x axis, 5 ms/box).

As can be seen, the FHC is capable of bi-directional exchange of reactive power with the grid.

5 | CONCLUSIONS

When EV chargers are providing V2G services, they can inject undesired distorted currents, especially if the grid voltage has harmonics. This article presents an easy-to-implement control strategy that reduces the current distortion caused by a specific voltage harmonic of the grid. As practical example, the proposed control strategy has been used to develop a FHC, which has been applied and validated on a scaled EV charger prototype. However, the control strategy proposed in this paper can be used to develop any other controller aimed at reducing the desired harmonic.

From the experimental results, the effectiveness of the proposed control is confirmed. In this sense, it has reduced the fifth harmonic component of the current by 76.34% in comparation with a traditional current control. In the same way, the THD has been reduced from 6.06% to 2.82%, compared to a traditional current control. Furthermore, it is concluded that the proposed control strategy enables exchanging active and reactive power with the grid with a suitable dynamic for V2G applications. In this sense, the proposed FHC control has been able to manage the exchanged power flows within a response time of 1ms. In addition, it can be highlighted that the proposed strategy allows developing a controller for harmonic reduction without adding extra volume or weight to the system.

This control is compatible with different G2V and V2G recharging methodologies, so in the future, it is intended to combine them. Besides, the degradation induced in the batteries when providing V2G services to the grid is gaining more and more interest. Therefore, in the future, an EV charging strategy will be developed focused on two objectives: battery degradation minimization and grid injected current distortion minimization.

6 | REFERENCES

[1] IPCC, "Special Report. Global Warming of 1.5 ºC," 2018. Available: https://www.ipcc.ch/sr15/.

[2] C. Filote *et al*, "Environmental impact assessment of green energy systems for power supply of electric vehicle charging station," *International Journal of Energy Research,* 2020. DOI: 10.1002/er.5678.

[3] European Commission and Directorate-General for Energy, “Clean energy for all Europeans,” 2019. Available: https://ec.europa.eu/energy/topics/energy-strategy/clean-energy-all-europeans_en.

[4] Communication from The Commission to the European Parliament, The European Council, The Council, The European economic and Social Committee and The Committee of the Regions, “The European Green Deal”, 2019. Available: https://eur-lex.europa.eu/legal-content/EN/TXT/?uri=CELEX%3A52019DC0640.

[5] V. S. Tabar and V. Abbasi, "Energy management in microgrid with considering high penetration of renewable resources and surplus power generation problem," *Energy,* vol. 189, pp. 116264, 2019. Available: http://www.sciencedirect.com/science/article/pii/S0360544219319590.

[6] M. R. Rapizza and S. M. Canevese, "Fast frequency regulation and synthetic inertia in a power system with high penetration of renewable energy sources: Optimal design of the required quantities," *Sustainable Energy, Grids and Networks,* vol. 24, pp. 100407, 2020. Available: http://www.sciencedirect.com/science/article/pii/S2352467720303386. DOI: https://doi.org/10.1016/j.segan.2020.100407.

[7] A. Fernández-Guillamón *et al*, "Power systems with high renewable energy sources: A review of inertia and frequency control strategies over time," *Renewable and Sustainable Energy Reviews,* vol. 115, pp. 109369, 2019. Available: http://www.sciencedirect.com/science/article/pii/S1364032119305775. DOI: https://doi.org/10.1016/j.rser.2019.109369.

[8] X. Han *et al*, "Optimal operations of energy storage systems in multi-application scenarios of grid ancillary services based on electricity price forecasting," *International Journal of Energy Research,* 2020. Available: https://doi.org/10.1002/er.6300. DOI: https://doi.org/10.1002/er.6300.

[9] I. Miri *et al*, "Electric vehicle energy consumption modelling and estimation—A case study," *International Journal of Energy Research,* vol. 45, *(1),* pp. 501-520, 2021. Available: https://doi.org/10.1002/er.5700. DOI: https://doi.org/10.1002/er.5700.

[10] M. A. Awadallah *et al*, "Impact of EV Charger Load on Distribution Network Capacity: A Case Study in Toronto," *Canadian Journal of Electrical and Computer Engineering,* vol. 39, *(4),* pp. 268-273, 2016. . DOI: 10.1109/CJECE.2016.2545925.

[11] Peng-Yong Kong and G. K. Karagiannidis, "Charging Schemes for Plug-In Hybrid Electric Vehicles in Smart Grid: A Survey," *Access,* vol. 4, pp. 6846-6875, 2016. Available: https://ieeexplore.ieee.org/document/7586042. DOI: 10.1109/ACCESS.2016.2614689.

[12] A. R. Bhatti *et al*, "A critical review of electric vehicle charging using solar photovoltaic," *International Journal of Energy Research,* vol. 40, *(4),* pp. 439-461, 2016. Available: https://search.datacite.org/works/10.1002/er.3472. DOI: 10.1002/er.3472.

[13] D. Strickland *et al*, "Feasibility study: investigation of car park-based V2G services in the UK central hub," *The Journal of Engineering,* vol. 2019, *(17),* pp. 3967-3971, 2019. Available: https://doi.org/10.1049/joe.2018.8230. DOI: https://doi.org/10.1049/joe.2018.8230.

[14] M. C. Mercan *et al*, "Economic model for an electric vehicle charging station with vehicle-to-grid functionality," *International Journal of Energy Research,* vol. 44, *(8),* pp. 6697-6708, 2020. Available: https://doi.org/10.1002/er.5407. DOI: https://doi.org/10.1002/er.5407.

[15] U. Rehman *et al*, "Network overloading management by exploiting the in-system batteries of electric vehicles," *International Journal of Energy Research,* vol. 45, *(4),* pp. 5866-5880, 2021. Available: https://doi.org/10.1002/er.6207. DOI: https://doi.org/10.1002/er.6207.

[16] G. Saldaña *et al*, "Electric Vehicle into the Grid: Charging Methodologies Aimed at Providing Ancillary Services Considering Battery Degradation," *Energies (Basel),* vol. 12, *(12),* pp. 2443, 2019. Available: https://search.proquest.com/docview/2316883122. DOI: 10.3390/en12122443.

[17] H. Liu *et al*, "Electric Vehicle Power Trading Mechanism Based on Blockchain and Smart Contract in V2G Network," *IEEE Access,* vol. 7, pp. 160546-160558, 2019. . DOI: 10.1109/ACCESS.2019.2951057.

[18] X. Chen *et al*, "Online Scheduling for Hierarchical Vehicle-to-Grid System: Design, Formulation, and Algorithm," *IEEE Transactions on Vehicular Technology,* vol. 68, *(2),* pp. 1302-1317, 2019. DOI: 10.1109/TVT.2018.2887087.

[19] G. Buja, M. Bertoluzzo and C. Fontana, "Reactive Power Compensation Capabilities of V2G-Enabled Electric Vehicles," *IEEE Transactions on Power Electronics,* vol. 32, *(12),* pp. 9447-9459, 2017. DOI: 10.1109/TPEL.2017.2658686.

[20] S. Amamra and J. Marco, "Vehicle-to-Grid Aggregator to Support Power Grid and Reduce Electric Vehicle Charging Cost," *Access,* vol. 7, pp. 178528-178538, 2019. Available: https://ieeexplore.ieee.org/document/8930487. DOI: 10.1109/ACCESS.2019.2958664.

[21] Y. Shang *et al*, "A centralized vehicle-to-grid scheme with distributed computing capacity engaging internet of smart charging points: Case study," *International Journal of Energy Research,* vol. 45, *(1),* pp. 841-863, 2021. Available: https://doi.org/10.1002/er.5967. DOI: https://doi.org/10.1002/er.5967.

[22] W. Kempton and J. Tomić, "Vehicle-to-grid power implementation: From stabilizing the grid to supporting large-scale renewable energy," *Journal of Power Sources,* vol. 144, *(1),* pp. 280-294, 2005. Available: http://www.sciencedirect.com/science/article/pii/S0378775305000212. DOI: https://doi.org/10.1016/j.jpowsour.2004.12.022.

[23] B. Han *et al*, "Three-stage electric vehicle scheduling considering stakeholders economic inconsistency and battery degradation," *IET Cyber-Physical Systems: Theory & Applications,* vol. 2, *(3),* pp. 102-110, 2017. Available: https://doi.org/10.1049/iet-cps.2017.0015. DOI: https://doi.org/10.1049/iet-cps.2017.0015.

[24] D. Luca de Tena and T. Pregger, "Impact of electric vehicles on a future renewable energy-based power system in Europe with a focus on Germany," *International Journal of Energy Research,* vol. 42, *(8),* pp. 2670-2685, 2018. Available: https://doi.org/10.1002/er.4056. DOI: https://doi.org/10.1002/er.4056.

[25] E. Samadani *et al*, "Li-ion battery performance and degradation in electric vehicles under different usage scenarios," *International Journal of Energy Research,* vol. 40, *(3),* pp. 379-392, 2016. Available: https://doi.org/10.1002/er.3378. DOI: https://doi.org/10.1002/er.3378.

[26] K. Uddin *et al*, "The viability of vehicle-to-grid operations from a battery technology and policy perspective," *Energy Policy,* vol. 113, pp. 342-347, 2018. Available: http://www.sciencedirect.com/science/article/pii/S0301421517307619. DOI: https://doi.org/10.1016/j.enpol.2017.11.015.

[27] M. Woody *et al*, "Strategies to limit degradation and maximize Li-ion battery service lifetime - Critical review and guidance for stakeholders," *Journal of Energy Storage,* vol. 28, pp. 101231, 2020. Available: http://www.sciencedirect.com/science/article/pii/S2352152X19314227. DOI: https://doi.org/10.1016/j.est.2020.101231.

[28] M. Sufyan *et al*, "Charge coordination and battery lifecycle analysis of electric vehicles with V2G implementation," *Electr. Power Syst. Res.,* vol. 184, pp. 106307, 2020. Available: http://www.sciencedirect.com/science/article/pii/S0378779620301139. DOI: https://doi.org/10.1016/j.epsr.2020.106307.

[29] Pooya Davar *et al,* "Control of Power Electronic Converters and Systems," vol. 2, chap. 13. Academic Press, 2018.

[30] A. Kalair *et al*, "Review of harmonic analysis, modeling and mitigation techniques," *Renewable and Sustainable Energy Reviews,* vol. 78, pp. 1152-1187, 2017. Available: http://www.sciencedirect.com/science/article/pii/S1364032117306226. DOI: https://doi.org/10.1016/j.rser.2017.04.121.

[31] Marek Jasiński *et al,* "Advanced and Intelligent Control in Power Electronics and Drives - Control of Grid Connected Converter (GCC) Under Grid Voltage Disturbances," chap. 3. Springer, 2014.

[32] A. Lucas *et al*, "Grid harmonic impact of multiple electric vehicle fast charging," *Electric Power Systems Research,* vol. 127, pp. 13-21, 2015. Available: http://www.sciencedirect.com/science/article/pii/S0378779615001534. DOI: https://doi.org/10.1016/j.epsr.2015.05.012.

[33] T. Ding *et al*, "Harmonic characteristics analysis of PWM-based electric vehicle chargers considering control strategy," in *18th International Conference on Harmonics and Quality of Power (ICHQP),* 2018, . DOI: 10.1109/ICHQP.2018.8378942.

[34] G. Zhao and Y. Yue, "Harmonic analysis and suppression of electric vehicle charging station," in *IEEE International Conference on Mechatronics and Automation (ICMA),* 2017. DOI: 10.1109/ICMA.2017.8015841.

[35] Clara Serrano *et al*, "An evaluation of V2G for distribution network harmonic suppression," in *Cired,* 2019, pp. 1-5.

[36] B. Runqing *et al*, "Research on double-close-loop fuzzy controlled SVPWM VSR for EV charger," in - *2011 4th International Conference on Power Electronics Systems and Applications,* 2011. DOI: 10.1109/PESA.2011.5982960.

[37] X. Gao *et al*, "A composite control strategy for suppressing the current harmonic at the grid side of V2G charger," in *2nd IEEE Advanced Information Management,Communicates,Electronic and Automation Control Conference (IMCEC),* 2018. DOI: 10.1109/IMCEC.2018.8469596.

[38] A. Tiwary *et al*, "A PFC Rectifier Based EV Charger for Harmonic Reduction," *IFAC-PapersOnLine,* vol. 52, *(4),* pp. 294-299, 2019. Available: http://www.sciencedirect.com/science/article/pii/S2405896319305518. DOI: https://doi.org/10.1016/j.ifacol.2019.08.214.

[39] A. Q. Ansari *et al*, "Algorithm for power angle control to improve power quality in distribution system using unified power quality conditioner," *IET Gener. Transm. Distrib.,* vol. 9, *(12),* pp. 1439-1447, 2015. Available: https://doi.org/10.1049/iet-gtd.2014.0734. DOI: https://doi.org/10.1049/iet-gtd.2014.0734.

[40] X. Wang *et al*, "Full Feedforward of Grid Voltage for Grid-Connected Inverter With LCL Filter to Suppress Current Distortion Due to Grid Voltage Harmonics," *IEEE Transactions on Power Electronics,* vol. 25, *(12),* pp. 3119-3127, 2010. DOI: 10.1109/TPEL.2010.2077312.

[41] S. Vinnakoti and V. R. Kota, "ANN based control scheme for a three-level converter based unified power quality conditioner," *Journal of Electrical Systems and Information Technology,* vol. 5, *(3),* pp. 526-541, 2018. Available:

http://www.sciencedirect.com/science/article/pii/S2314717218300060. DOI: https://doi.org/10.1016/j.jesit.2017.11.001.

[42] S. Vinnakoti and V. R. Kota, "Implementation of artificial neural network based controller for a five-level converter based UPQC," *Alexandria Engineering Journal,* vol. 57, *(3),* pp. 1475-1488, 2018. Available: http://www.sciencedirect.com/science/article/pii/S1110016817301205. DOI: https://doi.org/10.1016/j.aej.2017.03.027.

[43] G. N. Baltas *et al*, "Grid-Forming Power Converters Tuned Through Artificial Intelligence to Damp Subsynchronous Interactions in Electrical Grids," *IEEE Access,* vol. 8, pp. 93369-93379, 2020. DOI: 10.1109/ACCESS.2020.2995298.

[44] J. Heaton, "Artificial Intelligence for Humans. Deep Learning and Neural Networks," vol. 3. Heaton Research Inc, 2015.

[45] S. Jiang *et al*, "Active EMI Filter Design With a Modified LCL-LC Filter for Single-Phase Grid-Connected Inverter in Vehicle-to-Grid Application," *IEEE Transactions on Vehicular Technology,* vol. 68, *(11),* pp. 10639-10650, 2019. . DOI: 10.1109/TVT.2019.2944220.

[46] L. Zhang *et al*, "Research on power quality control method of V2G system of electric vehicle based on APF," in *International Conference on Advanced Mechatronic Systems (ICAMechS),* 2019. DOI: 10.1109/ICAMechS.2019.8861642.

[47] M. Zolfaghari *et al*, "Using V2G technology as virtual active power filter for flexibility enhancement of HVDC systems," in *IEEE 14th International Conference on Compatibility, Power Electronics and Power Engineering (CPE-POWERENG),* 2020. DOI: 10.1109/CPE-POWERENG48600.2020.9161602.

[48] T. Na *et al*, "Active power filter for single-phase Quasi-Z-source integrated on-board charger," *CPSS Transactions on Power Electronics and Applications,* vol. 3, *(3),* pp. 197-201, 2018. . DOI: 10.24295/CPSSTPEA.2018.00019.

[49] V. Monteiro *et al*, "Improved vehicle-for-grid (iV4G) mode: Novel operation mode for EVs battery chargers in smart grids," *International Journal of Electrical Power & Energy Systems,* vol. 110, pp. 579-587, 2019. Available: http://www.sciencedirect.com/science/article/pii/S0142061517329083. DOI: https://doi.org/10.1016/j.ijepes.2019.03.049.

[50] S. Taghizadeh *et al*, "A unified multi-functional on-board EV charger for power-quality control in household networks," *Applied Energy,* vol. 215, pp. 186-201, 2018. Available: http://www.sciencedirect.com/science/article/pii/S0306261918301259. DOI: https://doi.org/10.1016/j.apenergy.2018.02.006.

[51] A. Ramesh and H. Habeebullah Sait, "An approach towards selective harmonic elimination switching pattern of cascade switched capacitor twenty nine-level inverter using artificial bee colony algorithm," *Microprocessors and Microsystems,* vol. 79, pp. 103292, 2020. Available: http://www.sciencedirect.com/science/article/pii/S0141933120304518. DOI: https://doi.org/10.1016/j.micpro.2020.103292.

[52] S. Ahmad *et al*, "Selective harmonics elimination in multilevel inverter by a derivative-free iterative method under varying voltage condition," *ISA Trans.,* vol. 92, pp. 241-256, 2019. Available: http://www.sciencedirect.com/science/article/pii/S0019057819300837. DOI: https://doi.org/10.1016/j.isatra.2019.02.015.

[53] S. Bhadra and H. Patangia, "An analytical method of switching waveform design for selective harmonic elimination," *Math. Comput. Simul.,* vol. 184, pp. 41-54, 2021. Available: http://www.sciencedirect.com/science/article/pii/S0378475420301440. DOI: https://doi.org/10.1016/j.matcom.2020.04.018.

[54] C. Buccella *et al*, "Mathematical proof of a harmonic elimination procedure for multilevel inverters," *Math. Comput. Simul.,* vol. 184, pp. 69-81, 2021. Available: http://www.sciencedirect.com/science/article/pii/S0378475420302317. DOI: https://doi.org/10.1016/j.matcom.2020.07.003.

[55] S. Habib *et al*, "Assessment of electric vehicles concerning impacts, charging infrastructure with unidirectional and bidirectional chargers, and power flow comparisons," *International Journal of Energy Research,* vol. 42, *(11),* pp. 3416-3441, 2018. Available: https://doi.org/10.1002/er.4033. DOI: https://doi.org/10.1002/er.4033.

[56] A. Micallef *et al*, "Mitigation of Harmonics in Grid-Connected and Islanded Microgrids Via Virtual Admittances and Impedances," *IEEE Transactions on Smart Grid,* vol. 8, *(2),* pp. 651-661, 2017. DOI: 10.1109/TSG.2015.2497409.

[57] Guangkai Li *et al*, "Research of nonlinear control strategy for VSC-HVDC system based on Lyapunov stability theory," in *Third International Conference on Electric Utility Deregulation and Restructuring and Power Technologies,* pp. 2187-2191, 2008. DOI: 10.1109/DRPT.2008.4523773.

[58] J. K. Pradhan *et al*, "Small-signal modeling and multivariable PI control design of VSC-HVDC transmission link," *Electric Power Systems Research,* vol. 144, pp. 115-126, 2017. Available: http://www.sciencedirect.com/science/article/pii/S0378779616304801. DOI: https://doi.org/10.1016/j.epsr.2016.11.005.

[59] M. Ndreko *et al*, "Study on FRT compliance of VSC-HVDC connected offshore wind plants during AC faults including requirements for the negative sequence current control," *International Journal of Electrical Power & Energy Systems,* vol. 85, pp. 97-116, 2017. Available: http://www.sciencedirect.com/science/article/pii/S014206151630758X. DOI: https://doi.org/10.1016/j.ijepes.2016.08.009.

[60] Y. Zhou *et al*, "A Prototype of Modular Multilevel Converters," *IEEE Transactions on Power Electronics,* vol. 29, *(7),* pp. 3267-3278, 2014. DOI: 10.1109/TPEL.2013.2278338.

[61] S. B. Bashir and A. R. Beig, "An improved voltage balancing algorithm for grid connected MMC for medium voltage energy conversion," *International Journal of Electrical Power & Energy Systems,* vol. 95, pp. 550-560, 2018. Available: http://www.sciencedirect.com/science/article/pii/S0142061517309742. DOI: https://doi.org/10.1016/j.ijepes.2017.09.002.

[62] X. Wang *et al*, "New Repetitive Current Controller for PWM Rectifier," *IFAC-PapersOnLine,* vol. 51, *(4),* pp. 154-159, 2018. Available: http://www.sciencedirect.com/science/article/pii/S2405896318304154. DOI: https://doi.org/10.1016/j.ifacol.2018.06.118.

[63] O. A. Giddani *et al*, "Multi-task control for VSC–HVDC power and frequency control," *International Journal of Electrical Power & Energy Systems,* vol. 53, pp. 684-690, 2013. Available: http://www.sciencedirect.com/science/article/pii/S0142061513001944. DOI: https://doi.org/10.1016/j.ijepes.2013.05.002.

[64] Z. Yihua *et al*, "Research on Security and Stability Characteristics and Control Strategies of Power Grid with VSC-HVDC," *Energy Procedia,* vol. 145, pp. 351-356, 2018. Available: http://www.sciencedirect.com/science/article/pii/S1876610218300717. DOI: https://doi.org/10.1016/j.egypro.2018.04.063.

[65] M. H. Rashid, “Power Electronics Handbook”. Academic Press, 2001.

[66] R. Teichmann and S. Bernet, "A comparison of three-level converters versus two-level converters for low-voltage drives, traction, and utility applications," *IEEE Transactions on Industry Applications,* vol. 41, *(3),* pp. 855-865, 2005. DOI: 10.1109/TIA.2005.847285.

[67] Y. Zhang *et al*, "Review of modular multilevel converter based multi-terminal HVDC systems for offshore wind power transmission," *Renewable and Sustainable Energy Reviews,* vol. 61, pp. 572-586, 2016. Available: http://www.sciencedirect.com/science/article/pii/S1364032116001386. DOI: https://doi.org/10.1016/j.rser.2016.01.108.

[68] P. Vidal *et al*, "Generalized inverses applied to pulse width modulation for static conversion: A first study," in *15th European Conference on Power Electronics and Applications (EPE),* pp. 1-10, 2013. DOI: 10.1109/EPE.2013.6634683.

TABLE 1 Experimental setup

Symbol	Meaning	Value
F	frequency	50 Hz
V_g	grid voltage	400 V
V_{DC}	dc voltage source	600 V
L	filter inductance	7.4 mH
R	filter resistance	0.1 Ω
C	Dc bus capacitor	1 mF
f_{con}	commutation frequency	10 kHz
f_c	control signal frequency	20 kHz
P_N	converter nominal power	35 kW